

# Experimental demonstration of a unified framework for mixed-state geometric phases

J. ZHU<sup>1,2</sup>, M. SHI<sup>1(a)</sup>, V. VEDRAL<sup>4,5</sup>, X. PENG<sup>1</sup>, D. SUTER<sup>3</sup> and J. DU<sup>1(b)</sup>

<sup>1</sup> Hefei National Laboratory for Physical Sciences at Microscale and Department of Modern Physics, University of Science and Technology of China - Hefei, Anhui 230026, PRC

<sup>2</sup> Department of Physics and Shanghai Key Laboratory for Magnetic Resonance, East China Normal University Shanghai 200062, PRC

<sup>3</sup> Fakultät Physik, Technische Universität Dortmund - 44221 Dortmund, Germany, EU

<sup>4</sup> Department of Physics and Astronomy, University of Leeds - Leeds LS2 9JT, UK, EU

<sup>5</sup> Department of Physics, National University of Singapore - 2 Science Drive, Singapore

received 30 January 2011; accepted in final form 17 March 2011

published online 18 April 2011

PACS 03.67.-a – Quantum information

PACS 03.65.Vf – Phases: geometric; dynamic or topological

PACS 76.60.-k – Nuclear magnetic resonance and relaxation

**Abstract** – Geometric phases have been found in every major branch of physics and play an important role in mathematics and quantum computation. Here, we unify two proposed definitions of the geometric phase in mixed states —Uhlmann’s phase and Sjöqvist’s phase— in a new formalism based on interferometry and further provide an experimental demonstration in NMR. This is also the first experimental measurement of Uhlmann’s geometric phase.

Copyright © EPLA, 2011

When a quantum system undergoes a general physical evolution, its state acquires two phase factors, the dynamical and geometric phases. The latter is independent of the former and its value is only a function of the path described by the system throughout its evolution; in particular it does not depend on any details of the dynamics [1,2]. Geometric phases play an extremely important role in many different areas of physics. Originally discovered within the context of quantum mechanics and atom optics, their significance quickly became transparent in mathematical physics, condensed matter and high-energy physics [3]. Recently, they have also been used in quantum computation [4–7].

Most early works on the geometric phase focus on pure quantum states [8–11]. These, however, are very unrealistic and almost never occur in a real physical world. The definition of geometric phase for a mixed quantum state becomes difficult because of its reduced coherence. So far, two different methods are presented to try to define a geometric phase in mixed-state cases [12,13]. One was done by Uhlmann [12], using the fact that any mixed

state can be represented as a pure state in an extended Hilbert space. The other is due to Sjöqvist *et al.* [13], which provides an operationally well-defined notion of phase in interferometry [14,15]. These two definitions result in different values for the geometric phases for mixed states.

In this letter, we provide one new formalism of geometric phase for mixed states, which implies a unified framework for both methods. Moreover, using liquid-state NMR, we present an experimental demonstration of their unification. There are three important highlights in our present results. One is the first realization of Uhlmann’s geometric phase for mixed states. The second is the experimental comparison to the Sjöqvist phase. The third contribution is a unified theoretical framework for both phases.

As a unified setting for discussing geometric phases for mixed quantum states, we consider a system consisting of a spin  $S = 1/2$  coupled to an ancilla spin  $A = 1/2$ . We will assume that the complete system  $S \otimes A$  is always in a pure state, but if  $S$  and  $A$  are entangled, the  $S$ -subsystem is in a mixed state. Using this system, we present a formalism for geometric phases of mixed states that unifies the analysis of Sjöqvist *et al.* with that of Uhlmann. The difference between them can be traced to different evolutions of the ancilla spin.

<sup>(a)</sup>E-mail: shmj@ustc.edu.cn

<sup>(b)</sup>E-mail: djf@ustc.edu.cn

$$\gamma^U(t) = -\arctan \left[ \frac{(c_0^2 - c_1^2)(\cos \theta^s \tan \frac{\omega^s t}{2} + \cos \theta^a \tan \frac{\omega^a t}{2})}{1 + (\cos \theta^s \cos \theta^a + c_0 c_1 \sin \theta^s \sin \theta^a) \tan \frac{\omega^s t}{2} \tan \frac{\omega^a t}{2}} \right], \quad (2)$$

We write the initial state of the combined system  $S \otimes A$  as  $|\Psi\rangle = c_0|0\rangle^s|0\rangle^a + c_1|1\rangle^s|1\rangle^a$  with  $c_0$  and  $c_1$  being real positive numbers and satisfying  $c_0^2 + c_1^2 = 1$ . The reduced density operator of the system  $S$  is then  $\rho^s = c_0^2|0\rangle\langle 0| + c_1^2|1\rangle\langle 1|$ . Without loss of generality, we have thus chosen the basis states such that the system density operator of the initial state is diagonal and the ancilla states are “parallel” to those of the system.

The evolution of the combined system is determined by the propagator

$$U(t) = U^s(t) \otimes U^a(t) = e^{-iH^s t/\hbar} \otimes e^{-iH^a t/\hbar},$$

where  $H^s$  and  $H^a$  are time-independent Hamiltonians acting only on the subspace of the system and ancilla, respectively.

This framework covers the geometric phases of Sjöqvist and Uhlmann; the system behaves identically in the two cases, and we write the system Hamiltonian as  $H^s = -\vec{\omega}^s \cdot \vec{S}^s$ , where the magnetic field (in frequency units)  $\vec{\omega}^s$  acts only on the system spin and  $\vec{S}^s$  is the corresponding spin operator. The difference between the two geometric phases can be traced to the difference in the Hamiltonians  $H^a = -\vec{\omega}^a \cdot \vec{S}^a$  considered for the ancilla subsystem.

*Case 1. Sjöqvist phase:* In Sjöqvist’s definition of the mixed-state geometric phase, the magnetic field acting on the ancilla is chosen such that under the evolution  $|\Psi(t)\rangle = [U^s(t) \otimes U_{\text{Sj}ö}^a(t)]|\Psi\rangle$  the states  $|0\rangle^s|0\rangle^a$  and  $|1\rangle^s|1\rangle^a$  are parallel transported, *i.e.* the ancilla Hamiltonian cancels the dynamical phase contribution of the system Hamiltonian. This is fulfilled by the choice of  $H_{\text{Sj}ö}^a = -\omega^a S_z^a$ , where  $\omega^a = -\omega^s \cos \theta^s$  and  $\theta^s$  is the angle between the direction of the field acting on the system and the  $z$ -axis. For the complete system  $S \otimes A$ , the evolution corresponds then to parallel transport, and the resulting geometric phase of the two-qubit state,  $\arg[\langle \Psi | U^s(t) \otimes U_{\text{Sj}ö}^a(t) | \Psi \rangle]$ , is equal to Sjöqvist’s phase for the mixed state of the subsystem  $S$ ,

$$\gamma^S(t) = \arg \sum_{j=0}^1 c_j^2 |{}^s\langle j | U^s(t) | j \rangle^s| e^{i\beta_j(t)}, \quad (1)$$

where  $\beta_j(t)$  is the geometric phase associated with  $|j\rangle^s$  under the evolution  $U^s(t)$ .

*Case 2. Uhlmann phase:* Uhlmann’s version of the geometric phase can be obtained if the ancilla Hamiltonian fulfills the following conditions: i)  $\omega^a \cos \theta^a + \omega^s \cos \theta^s = 0$  and ii)  $\tan \theta^a = 2c_0 c_1 \tan \theta^s$ . Here,  $\theta^a$  is the angle between the direction of the field acting on the ancilla and the  $z$ -axis, and  $\theta^s$  is the one for the field acting on the system qubit. These two conditions are the concrete form of the

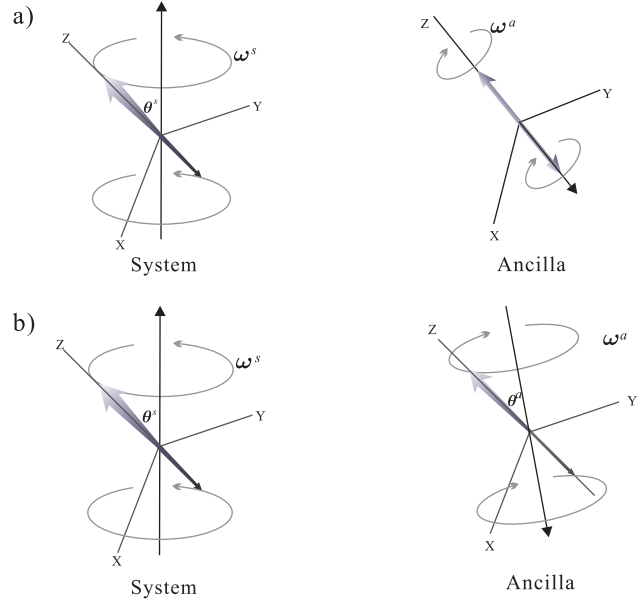


Fig. 1: (Color online) Comparison of the two types of evolution of system and ancilla that lead to the two different geometric phases. Two pure components of the system’s mixed state are represented by two arrows along the  $z$ -axis. The fixed magnetic field  $\mathbf{B}^s$  lies in the  $xz$ -plane, at an angle  $\theta^s$  from the  $z$ -axis. The system qubit rotates around  $\mathbf{B}^s$  with angular frequency  $\omega^s$ . The upper figure a) corresponds to case 1, in which the magnetic field for the ancilla is  $\mathbf{B}^a = -e_z B^s \cos \theta^s$ . The lower figure b) corresponds to case 2 (Uhlmann phase).

results obtained in [15]. Condition i) ensures that  $|\Psi(t)\rangle$  is parallel transported. It is just the condition required for the Sjöqvist phase. To obtain the Uhlmann phase, we further need condition ii). In this case, the transformation  $U^s(t) \otimes U_{\text{Uhl}}^a(t)$  results in a total phase difference, *i.e.*,  $\arg[\langle \Psi | U^s(t) \otimes U_{\text{Uhl}}^a(t) | \Psi \rangle]$ , which is equal to the Uhlmann phase

*see eq. (2) above*

where  $\omega^s = \gamma B^s$  is the precession frequency of the system nuclei in magnetic field  $\mathbf{B}^s$  and similarly for  $\omega^a$ , and without loss of generality we let  $c_1 > c_2$ . Figure 1 compares the two cases: the left-hand part shows the orientation of the field acting on the system, the right-hand part for the ancilla.

Figure 2 shows how the geometrical phase acquired by the system during one cycle depends on the orientation  $\theta^s$  of the system field and the purity  $r$  in Uhlmann’s definition (left) and Sjöqvist’s definition (right). The two definitions agree in the limiting case of a pure state ( $r = 1$ ), but they diverge rapidly for  $r < 1$  and reach different limiting values

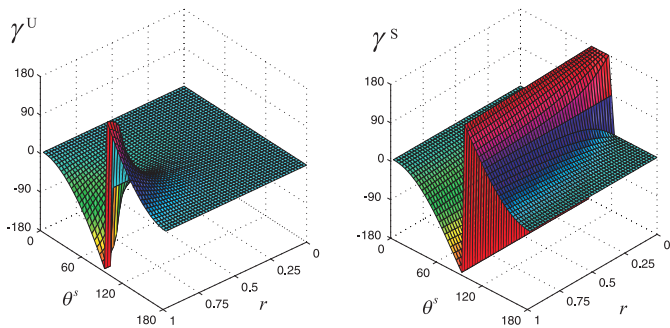


Fig. 2: (Color online) The Uhlmann's geometric phase  $\gamma^U$  (left) and the Sjöqvist's geometric phase  $\gamma^S$  (right) as a function of purity  $r$  and angle  $\theta^s$ . All angles are in degrees.

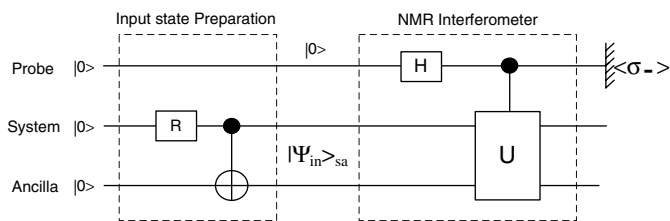


Fig. 3: The quantum network for observing the geometric phase using NMR interferometry. Probe qubit (denoted by  $p$ ) is used to measure the geometric phase. The pseudo-Hadamard gate  $H^p = e^{-i\frac{\pi}{2}S_y^p}$  puts the probe qubit into an equal superposition state, acting as a symmetric beam splitter. Another single-qubit rotation  $R^s = e^{-i\phi S_y^s/\hbar}$  with  $\phi = 2\arccos(c_0)$  and a controlled-NOT gate prepare system and ancilla into an entangled state  $|\Psi_{in}\rangle^{sa}$ .  $U$  represents a bilocal unitary transformation for either the Uhlmann phase or the Sjöqvist phase (see the text for details), performed on the input state  $|\Psi_{in}\rangle^{sa}$  conditionally on the state of the probe qubit.

for  $r \rightarrow 0$ : in the Uhlmann case, it is always 0, but in the Sjöqvist case, it tends towards 0 or  $\pi$ .

Having presented the unified picture of two phases of the mixed state, we can also observe them in a unified experimental setting: we measure the geometric phase acquired by the system qubit during an evolution around a closed cycle. Since the phase change of the state is not directly observable, we need an interferometric measurement that makes the phase change visible. Here, we choose nuclear magnetic resonance (NMR) interferometry [16], where the two paths of the interferometer correspond to the two states of a probe qubit.

Figure 3 summarizes the experimental procedure: in order to obtain a purification of the initial system state  $\rho^s$ , we introduce an ancilla qubit  $A$  and start from the product state  $|0\rangle^s \otimes |0\rangle^a$ . A rotation  $R$  is applied on system state  $|0\rangle^s$ , followed by a controlled-NOT gate on  $S \otimes A$ . The rotation  $R$  is given by  $R = \exp[-i\phi S_y^s/\hbar]$  where  $S_y^s$  is the  $y$ -component of system spin and  $\phi = 2\arccos(c_0)$ . The probe qubit is initialized into an equal-weight superposition  $(|0\rangle_p + |1\rangle_p)/\sqrt{2}$  by applying a Hadamard gate to the  $|0\rangle_p$  state. Then a conditional rotation generates a unitary evolution  $U$  of the ‘‘copy’’ of the  $|\Psi_{in}\rangle^{sa}$  state that

is connected to the  $|1\rangle_p$  state. Here  $U$  is a bilocal unitary evolution and can be either  $U^s(t) \otimes U_{\text{Sj}ö}^a(t)$  for the Sjöqvist phase (case 1) or  $U^s(t) \otimes U_{\text{Uhl}}^a(t)$  for the Uhlmann phase (case 2). As a result of this operation, the system is in the state  $(|0\rangle_p \otimes |\Psi_{in}\rangle^{sa} + |1\rangle_p \otimes U|\Psi_{in}\rangle^{sa})/\sqrt{2}$ , so that the probe qubit is in the state  $[I + \text{Re}[{}^{sa}\langle\Psi_{in}|U|\Psi_{in}\rangle^{sa}]\sigma_x^p + \text{Im}[{}^{sa}\langle\Psi_{in}|U|\Psi_{in}\rangle^{sa}]\sigma_y^p]/2$ , where  $\sigma_k$  ( $k = x, y, z$ ) are Pauli matrices and spin operators are expressed as  $S_k = \hbar\sigma_k/2$ . By measuring the expectation value  $\langle\sigma_-^p\rangle = \langle\sigma_x^p - i\sigma_y^p\rangle$  of the probe qubit, we obtain the geometric phase,  $\arg(\langle\Psi_{in}|U|\Psi_{in}\rangle) = \arg\langle\sigma_-^p\rangle$ .

The molecule ( $^{13}\text{C}$ -labelled alanine) used for this experiment contains three  $^{13}\text{C}$  spin- $\frac{1}{2}$  nuclei as qubits. The Hamiltonian of the 3-qubit system is (in angular-frequency units)  $H = \sum_{i=1}^3 \omega_i S_z^i + 2\pi \sum_{i<j}^3 J_{ij} S_z^i S_z^j$  with the Larmor angular frequencies of the  $i$ -th spin  $\omega_i$ ,  $\omega_1 = 17740$ ,  $\omega_2 = 1676.7$ ,  $\omega_3 = 5128.2$ , and spin-spin coupling constants  $J_{13} = 54.1$  Hz,  $J_{23} = 34.9$  Hz,  $J_{12} = -1.3$  Hz. Qubits 1, 2 and 3 are used as the probe qubit, system qubit, and ancillary qubit, respectively. Experiments were performed at room temperature using a standard 400 MHz NMR spectrometer (AV-400 Bruker instrument).

The system was first prepared in a pseudo-pure state (PPS)  $\rho_{000} = \frac{1-\epsilon}{8}\mathbb{1} + \epsilon|000\rangle\langle 000|$ , where  $\epsilon \approx 10^{-5}$  describes the thermal polarization of the system and  $\mathbb{1}$  is a unit matrix, using the method of spatial averaging [17]. From the state  $\rho_{000}$ , we prepared the input state  $\rho_{in} = \frac{1-\epsilon}{8}\mathbb{1} + \epsilon|0\rangle_1|\Psi_{in}\rangle_{sa}\langle\Psi_{in}|_1\langle 0|$  with a rotation and a CNOT gate. The probe qubit 1 was then put into a superposition state by another Hadamard gate. The physical evolutions were implemented by rotating the system qubit and ancilla qubit in the magnetic fields  $\mathbf{B}^s$  and  $\mathbf{B}^a$ , respectively, conditioned on the state of the probe qubit. We set  $\omega^s t = \mu B^s t = 2\pi$  so that the system qubit undergoes a cyclic evolution, *i.e.*  $U^s = -\mathbb{1}$ , a negative unit operator. Therefore in the experiment, we only implemented a conditional rotation  $U^a$  on the ancilla, where  $U^a = U_{\text{Sj}ö}^a$  and  $U^a = U_{\text{Uhl}}^a$  for observing the Sjöqvist and Uhlmann phases, respectively. In contrast to a positive unit operator, the negative unit operator  $U^s$  in experiment only caused a  $\pi$  phase difference between the measured and theoretical geometric phase, *i.e.*,  $\gamma^{ex} = \pi + \gamma^{th}$ .

In order to improve the quantum coherent control, experimentally all single-qubit gates were implemented as robust strongly modulating pulses (SMP) [18–20]. We calculated these gate operations by maximizing the gate fidelity of the simulated propagator (*i.e.* its overlap with the ideal gate). To reduce the sensitivity to RF field inhomogeneities, the fidelity was averaged over a weighted distribution of radio frequency (RF) field strengths. We found optimal solutions for SMPs with pulse durations of 200–500  $\mu\text{s}$ , with calculated gate fidelities  $> 0.995$ . The quantum circuit of fig. 3 was realized with a sequence of these local SMPs separated by time intervals of free evolution under the Hamiltonian. The overall theoretical fidelity of this pulse sequence is about 0.98.

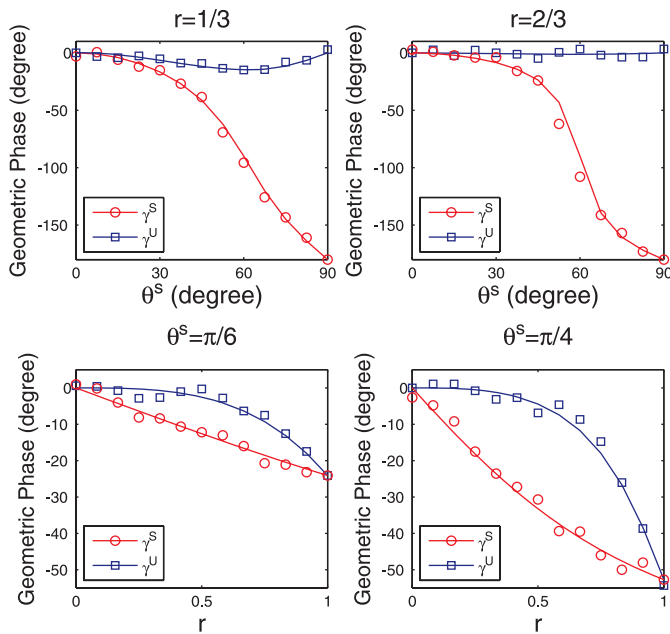


Fig. 4: (Color online) Experimental values for Uhlmann's geometric phases  $\gamma^U$  (denoted by blue squares) and Sjöqvist's geometric phases  $\gamma^S$  (denoted by red circles). Theoretical values are represented by smooth curves. The variability in the experimental points (estimated by repetition) is about  $\pm 3^\circ$ .

The phase detection requires the measurement of the complex signal,  $\langle \sigma_-^p \rangle$ , containing the  $x$  and  $y$  components. In fact, in any NMR experiment, this complex signal  $\langle \sigma_-^p \rangle(t)$  corresponds to the complex free induction decay (FID), obtained by the simultaneous observation of both  $x$  and  $y$  components by quadrature detection. This signal was subjected to a complex Fourier transformation to obtain the complex spectrum, thereby separating the signal of the three qubits. The geometric phase  $\gamma_g = \arctan(\text{Int}_{\text{Im}}/\text{Int}_{\text{Re}})$  was determined by integrating the real and imaginary part of the spectrum,  $\text{Int}_{\text{Im}}$  and  $\text{Int}_{\text{Re}}$ .

We measured both the Sjöqvist phase  $\gamma^S$  (using the unitary cyclic evolution of the ancilla  $U_{\text{Sj}}^a(r, \theta^s)$ ) and the Uhlmann phase  $\gamma^U$  (using the unitary cyclic evolution of the ancilla  $U_{\text{Uhl}}^a(r, \theta^s)$ ) for mixed states of varying purity  $r$  and varying angle of the magnetic field  $\theta^s$ . Two separate sets of experiments were performed: in the first one, we varied the purity  $r$  from 0 to 1 with a fixed the angle of the magnetic field  $\theta^s$  (we chose two values of  $\theta^s = \pi/6$  and  $\theta^s = \pi/4$  in the experiments). In the other, we varied the angle  $\theta^s$  from 0 to  $\pi/2$  while keeping the purity  $r$  fixed (likewise, two values of  $r = 1/3$  and  $2/3$  were chosen in the experiments). Data were collected for 13 equidistant values of the variable parameter, either the purity  $r$  or the angle  $\theta^s$ .

Figure 4 shows the experimental results for these four situations. Clearly, the measured Sjöqvist and Uhlmann phases are in excellent agreement with the theoretical

expectation (see fig. 2). The deviation between the experimental and theoretical values is primarily due to the inhomogeneity of the radio frequency field and the static magnetic field, imperfect calibration of radio frequency pulses, and signal decay during the experiments.

In conclusion, we have experimentally observed the Uhlmann's and Sjöqvist's geometric phases for mixed states with different purity. Also we found these two different definitions of mixed-state geometric phases resulting from different choices of the representation of the Hilbert space of the ancilla, which is in accordance with the theoretical prediction. Our work raises a number of possible interesting future directions. Firstly, it seems that we can obtain other definitions for the mixed-state geometric phase, different from the Uhlmann phase and the Sjöqvist phase, by suitably tailoring the interaction with the ancilla. Secondly, it may be that some of these geometric phases are more robust than others, in which case, they are worth learning about. Thirdly, more fundamentally, we should consider what happens if we cannot access the ancilla [21–23]. Is the notion of mixed-state geometric phase then to be abandoned, or —more likely— can we still use some references with respect to which the geometric phase could be defined?

\*\*\*

This work was supported by the National Natural Science Foundation of China, the CAS, Ministry of Education of PRC, and the National Fundamental Research Program. VV acknowledges the Wolfson Foundation and the Royal Society as well as the Engineering and Physical Science Research Council in UK.

## REFERENCES

- [1] PANCHARATNAM S., *Proc. Indian Acad. Sci., Sect. A*, **44** (1956) 247.
- [2] BERRY M. V., *Proc. R. Soc. London, Ser. A*, **392** (1984) 45.
- [3] SHAPER A. and WILCZEK F., *Geometrical Phases in Physics* (World Scientific) 1990.
- [4] ZANARDI P. and RASETTI M., *Phys. Lett. A*, **264** (1999) 94.
- [5] DUAN L. M., CIRAC J. I. and ZOLLER P., *Science*, **292** (2001) 1695.
- [6] JONES J. A., VEDRAL V., EKERT A. and CASTAGNOLI G., *Nature (London)*, **403** (2000) 869.
- [7] FALCI G., FAZIO R., MASSIMO PALMA G., SIEWERT J. and VEDRAL V., *Nature (London)*, **407** (2000) 355.
- [8] AHARONOV Y. and ANANDAN J., *Phys. Rev. Lett.*, **58** (1987) 1593.
- [9] SAMUEL J. and BHANDRI R., *Phys. Rev. Lett.*, **60** (1988) 2339.
- [10] MUKUNDA N. and SIMON R., *Ann. Phys. (N.Y.)*, **228** (1993) 205.
- [11] PATI A. K., *Phys. Lett. A*, **202** (1995) 40.
- [12] UHLMANN A., *Rep. Math. Phys.*, **24** (1986) 229.

- [13] SJÖQVIST E. *et al.*, *Phys. Rev. Lett.*, **85** (2000) 2945.
- [14] DU J. *et al.*, *Phys. Rev. Lett.*, **91** (2003) 100403.
- [15] MARIE ERICSSON *et al.*, *Phys. Rev. Lett.*, **94** (2005) 1050401.
- [16] SUTER D., MUELLER K. and PINES A., *Phys. Rev. Lett.*, **60** (1988) 1218.
- [17] CORY D. G., PRICE M. D. and HAVEL T. F., *Physica D: Nonlin. Phenom.*, **120** (1998) 82.
- [18] FORTUNATO E. *et al.*, *Chem. Phys.*, **116** (2002) 7599.
- [19] PRAVIA M. A. *et al.*, *J. Chem. Phys.*, **119** (2003) 9993.
- [20] MAHESH T. S. and SUTER D., *Phys. Rev. A*, **74** (2006) 062312.
- [21] CAROLLO A., FUENTES-GURIDI I., FRANCA SANTOS M. and VEDRAL V., *Phys. Rev. Lett.*, **90** (2003) 160402.
- [22] TONG D. M., SJÖQVIST E., KWEK L. C. and OH C. H., *Phys. Rev. Lett.*, **93** (2004) 080405.
- [23] ERICSSON M., PATI A. K., SJÖQVEST E., BRÄNNLUND J. and OI D. K. L., *Phys. Rev. Lett.*, **91** (2003) 090405.